J. Eur. Opt. Society-Rapid Publ. 2026, **22**, 55

https://doi.org/10.1051/jeos/2026050
Available online at: https://jeos.edpsciences.org

Journal of the European Optical Society-Rapid Publications

Recent Advances on Optics and Photonics 2026
Guest editors: Manuel Filipe P. C. M. Costa, Rogerio Nogueira and Alessandro Fantoni

Research Article — Open Access

Compact continuous-wave mid-infrared generation via a shared-cavity Nd:YVO_4/PPMgLN OPO with laser-diode pumping

Yi-Ping Wang[1,2], Shi-Chuang Jiang[1,2], Dong Sun[1,2], Hong Liu[1,2], Liang-Qin Gan[1,2], Hong-Kai Nian[3], and Hong-Yi Lin[1,2,*]

[1] School of Optoelectronic and Communication Engineering, Xiamen University of Technology, Xiamen 361024, PR China
[2] Fujian Key Laboratory of Optoelectronic Technology and Devices, Xiamen University of Technology, Xiamen 361024, PR China
[3] Fujian Zhengtai Judicial Expertise Center, Xiamen 361006, PR China

Received 31 March 2026 / Accepted 5 June 2026

Abstract. Compact mid-infrared laser generation is achieved using a demonstrated shared-cavity optical parametric oscillator (OPO) based on periodically poled magnesium-doped lithium niobate (PPMgLN). The shared-cavity design co-resonates the 1064 nm fundamental light and the ~1.5 μm signal wave within a single optical cavity, thereby ensuring good spatial mode overlap and intracavity power enhancement. This configuration substantially lowers the oscillation threshold and enhances the overall conversion efficiency. The oscillation threshold at 807.6 nm is only 0.9 W. Under stable operation at a 5.0 W pump power, the system generates output at 1472.9 nm (signal) and 3833.2 nm (idler), with respective output powers of 430 mW and 187 mW. Signal linewidth is 0.9 nm, while the idler linewidth is relatively wide, 6.4 nm. The generated 3.8 μm mid-infrared laser falls within the molecular "fingerprint" region – making it highly valuable for high-sensitivity spectral analysis and trace-gas sensing – while the 1.5 μm signal wavelength lies within the low-loss telecommunications window.

Keywords: Optical parametric oscillator, Shared cavity, Mid-infrared laser, PPMgLN.

1 Introduction

The mid-infrared spectral region – conventionally defined as 2–20 μm – encompasses the fundamental vibrational absorption bands of numerous gas molecules and is therefore widely regarded as the "molecular fingerprint region" [1]. It holds significant application potential in fields such as trace gas detection, environmental monitoring, biomedical diagnostics, industrial process analysis, and optoelectronic countermeasures [2, 3]. Of particular significance is the 3–5 μm atmospheric transmission window, which offers favorable propagation characteristics and therefore constitutes an optimal spectral band for developing high-sensitivity spectroscopic techniques [4–6]. The 1.5 μm wavelength band – widely adopted in optical communications – offers several distinct advantages, including low-loss transmission through standard optical fibers, mature and highly sensitive detector technology, and intrinsic eye safety [7]. These attributes render it exceptionally well suited for applications such as lidar systems, free-space optical communication, and fiber-optic sensing [8, 9]. As a pivotal technology for generating coherent mid-infrared radiation, OPOs derive their appeal from three key attributes: broad spectral tunability, high output power, and a fully solid-state architecture. These features have fueled extensive research and sustained technological advancement [10, 11].

Traditional OPO systems commonly adopt a discrete-cavity configuration, wherein the fundamental light resonator and the OPO cavity operate independently [12]. This design leads to structural complexity, challenges in spatial mode matching, limited system stability, and elevated costs. To overcome these limitations, shared-cavity OPO architectures have emerged. In such configurations, both the fundamental light and the signal wave resonate within a single common cavity – enabling precise spatial mode overlap and intracavity power enhancement [13]. Consequently, optical conversion efficiency is significantly improved, oscillation threshold is reduced, optical layout is greatly simplified, and overall system stability is enhanced. Meanwhile, the choice of pump source critically influences system reliability, cost, and integration capability. With c-mount packaging and beam shaping, laser diodes deliver high electro-optical efficiency, superior thermal management, stable beam quality, and cost-effectiveness, making them the ideal pump source for compact, robust, and economical all-solid-state mid-infrared OPO systems. This paper proposes and develops a shared-cavity

* Corresponding author: 2010111010@xmut.edu.cn

OPO system based on a c-mount LD pump source and PPMgLN as the nonlinear crystal. The output characteristics of the system at two distinct wavelength bands – 1.5 μm and 3.8 μm – are systematically investigated.

2 Experimental setup

Schematic diagram of the experimental setup is shown in Figure 1. An 807.6 nm c-mount LD is adopted as the pump source. This LD, combined with a fiber-based beam shaping and focusing configuration, uses a fiber to homogenize and condition the raw output beam into a uniform and stable near-Gaussian spot, greatly improving the spatial quality and pointing stability of the pump light. At the same time, this structure achieves efficient heat dissipation through c-mount packaging, supporting the stable operation of the LD at high power. Compared to the structure utilizing a fiber-coupled LD array, the present design offers greater compactness and simplicity.

The laser medium is a Nd:YVO_4 crystal with a size of 3 × 3 × 5 mm^3 and 0.2 at. % Nd^{3+}-doping. The left side of the crystal, M_{in}, is coated with an 807.6 nm high-transmission (HT) coating ($T > 98\%$) and a 1064 nm, 1.4–1.6 μm high-reflection (HR) coating ($R > 99\%$). The right side of the crystal is coated with a 1064 nm, 1.4–1.6 μm anti-reflection (AR) coating ($R < 0.5\%$). The output mirror, M_{oc}, has a radius of curvature of 100 mm. Its left side is coated with a 1064 nm HR coating ($R > 99\%$), a 1.4–1.7 HR coating ($R = 98\%$), and a 3–4 μm AR coating. The right side is coated with a 1.4–1.6 μm and 3–4 μm HT coating. The material of the output mirror is CaF_2, which has a relatively small absorption coefficient in the mid-infrared range, facilitating the output of mid-infrared idler light. Both M_{in} and M_{oc} have the HR coating at 1064 nm, forming a resonant cavity for the fundamental light at 1064 nm; they also have the HR coating for the signal light, forming a resonant cavity for the OPO system. The resonant cavity length is 65 mm, and the total length including the LD is only 70 mm.

The PPMgLN crystal is 50 mm in length, and both sides are coated with a 1.4–1.6 μm and 3–4 μm HT coating. The thickness of the PPMgLN crystal is 1 mm. The PPMgLN crystal is mounted on a copper heat sink with a thermoelectric cooler (TEC) maintaining a setpoint of 25 ± 0.1 °C, and the MgO doping can effectively suppresses photorefractive damage under our experimental conditions. We selected five periods of 28.6, 28.8, 29.0, 29.2, and 28.4 μm, which can achieve tuning of the signal light from 1435 to 1473 nm and the idler light from 4114 to 3833 nm.

The shared-cavity OPO resonates both the fundamental and signal lights within a single optical cavity, leading to a fundamental enhancement in system performance. This architecture not only significantly increases the intracavity power of the fundamental light – thereby providing stronger driving power for nonlinear conversion – but also, and more importantly, ensures perfect spatial mode matching between the two beams. Across the entire cavity, especially within the nonlinear crystal, the spot sizes and wavefront curvatures of the fundamental and signal modes are automatically aligned. This enables highly efficient parametric oscillation and fundamentally overcomes the conversion-efficiency limitations imposed by mode mismatch in conventional external-cavity designs.

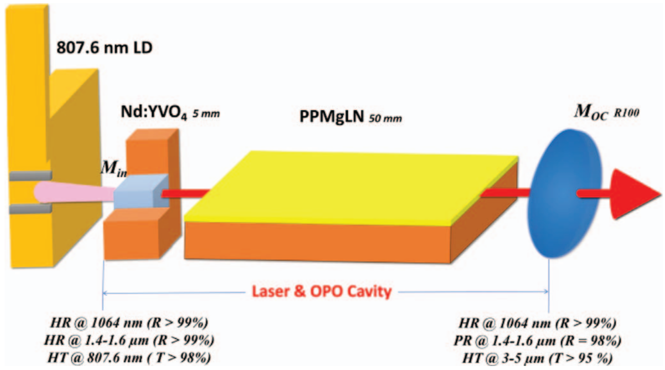

Figure 1. Schematic diagram of the experimental setup.

In terms of mechanical structure, all beams share the same cavity mirrors and mechanical mounts, which greatly reduces sensitivity to vibration, thermal drift, and mechanical misalignment. This configuration endows the system with good short-term stability over a two-hour period and beam pointing stability. Meanwhile, the inherent mode-selection property of the resonator guarantees that the output signal beam possesses a narrow spectral linewidth. This structure is simple and compact, providing a compact and low-cost architecture for mid-infrared continuous-wave lasers.

Using ABCD matrix analysis [14–16], the fundamental mode waist radius at the plane mirror M_{in} is calculated to be 122 μm in the cold cavity as shown in Figure 2. The measured LD spot radius at 807.6 nm is about 100 μm, giving an overlap integral of approximately 0.96, which confirms excellent mode matching at 1064 nm. Under high-power pumping, thermal lenses in both Nd:YVO_4 and PPMgLN are considered [17]. At 5.0 W pump power, the calculated thermal focal lengths are 48 mm and 96 mm, respectively. Including these thermal lenses, the waist radius at M_{in} decreases to 105 μm, still well above 100 μm, and the fundamental overlap integral reaches approximately 0.99. The cavity stability parameter remains between 0.21 and 0.35 for all pump powers (0–5.0 W), far below the stability limit of 1. For the signal light, taking 1500 nm as an example, at the pump power of 0 W, at the center of the PPLN crystal, the beam waists of the fundamental and signal lights are 124 μm and 147 μm, respectively, with an overlap integral of 0.97. At the pump power of 5.0 W, the corresponding beam waists become 130 μm and 108 μm, with an overlap integral of 0.96. Over the all pump powers (0–5.0 W), the signal beam waist remains less than the actual fundamental beam waist, maintaining good mode matching.

3 Results and discussion

3.1 Output spectral characteristics

Firstly, when the PPMgLN's period is 29.4 μm, under different pump powers (1.0, 3.0 and 5.0 W), we used the Yokogawa AQ6370 (resolution 0.02 nm) optical spectrum analyzer to measure the output spectra of the fundamental and signal lights of the OPO system as shown in Figure 3. With the increase of pump power, the output intensity of the fundamental light at 1063.9 nm remains basically unchanged, while the intensity of the signal light at 1472.9 nm increases significantly. During the nonlinear conversion operation of the OPO system, the power of the fundamental light in the cavity is always maintained near the oscillation threshold. When the externally injected pump energy increases, any additional pump energy is not used to further enhance the intensity of the fundamental light in the cavity, but is almost entirely used to drive the parametric down-conversion OPG process, efficiently converting into signal light at 1472.9 nm and idler light, and outputting through the output mirror to the outside of the cavity.

Then, we measure the output spectra of the signal and idler lights of the OPO system using a mid-infrared spectrometer (Bristol 771 Spectrum Analyzer, resolution 4 GHz), when the PPMgLN's period is 29.4 μm, as shown in Figure 4. The wavelength of the signal light is 1472.9 nm, and that of the idler light is 3833.2 nm. The linewidth of the fundamental light is 1.8 nm, and that of the signal light is 0.9 nm. Interestingly, the linewidth of the idler light is relatively wide, approximately 6.4 nm. In this OPO system, the asymmetry in the linewidths of the fundamental, signal, and idler lights originates from the differences in their mode selection and gain mechanisms within the resonant cavity. In this study, the signal light is designed as an intracavity resonant mode, and its wavelength is constrained by the longitudinal mode structure of the optical OPO cavity. The high reflectivity of the cavity mirrors and the multiple round-trip interference effect significantly narrow its linewidth and improve its spectral purity. In contrast, the gain of the idler light does not come from resonant amplification but is entirely dependent on the parametric down-conversion process in the nonlinear crystal.

The output wavelengths of the signal light and the idler light are very stable, as shown in Figure 5. Within a two-hour period, the signal light varies between 1472.79 nm and 1473.03 nm, with a fluctuation range of only 0.24 nm, while the idler light varies between 3832.51 nm and 3834.25 nm, with a fluctuation range of only 1.74 nm.

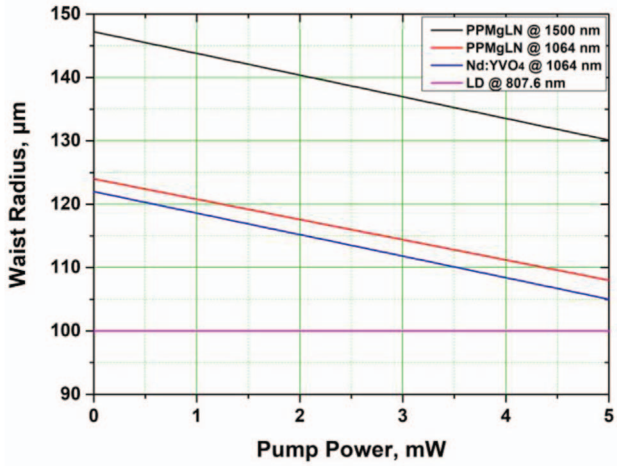

Figure 2. LD, fundamental and signal beam waists vs. pump power (0–5.0 W).

3.2 Parasitic visible light

We also measure the output spectra of parasitic visible light, pump light and signal light using a micro fiber optic spectrometer (Avantes AvaSpec-2048FT-SPU), as shown in Figure 6. In the visible light section, visible lights at 532.0 nm, 616.6 nm and 736.5 nm appear. Actually, the green light at 532.0 nm is the second harmonic of the fundamental light at 1063.9 nm, the red light at 736.5 nm is the second harmonic of the signal light at 1472.9 nm, while the orange light at 616.6 nm is the sum frequency of the fundamental and signal lights [18]. In this OPO system, the relative intensities of the visible lights (second harmonic and sum frequency) are mainly determined by the field intensities of the corresponding nonlinear processes and the degree of phase matching optimization. Among them, the sum frequency of the fundamental and signal lights is usually the strongest, as it is driven by the strongest fundamental and signal lights in the shared cavity and its phase matching condition is often associated with the tuning of the main parametric process, making it easy to achieve a high conversion efficiency [19]. The second harmonic of the fundamental light is often weaker, as the phase matching of this process is actively suppressed during the OPO design stage through crystal period to avoid energy loss of the fundamental light and ensure the efficiency of parametric down-conversion. The second harmonic of the signal light has the weakest intensity, although it is driven by a strong signal light, its phase matching condition is independent of the main OPO design and is usually not in the optimal state. These parasitic visible lights reduce the energy of both the fundamental and signal lights.

The total power of visible light is low, with a maximum power of only 30 mW. Although the power is very low, it can still affect the stability of the signal light power. The total parasitic power is less than 1% of the pump power, confirming a negligible impact on the overall conversion efficiency. Possible suppression strategies include: designing the poling period to detune parasitic phase-matching, inserting anti-reflection coatings for visible wavelengths inside the cavity, or moderately reducing the pump focusing. In the present work, no extra suppression is applied because the parasitic power is already negligible.

3.3 Output power characteristics

We measure the output powers of the signal light, idler light and total OPO under different pump powers, as shown in Figure 7. The threshold of the OPO system at 807.6 nm

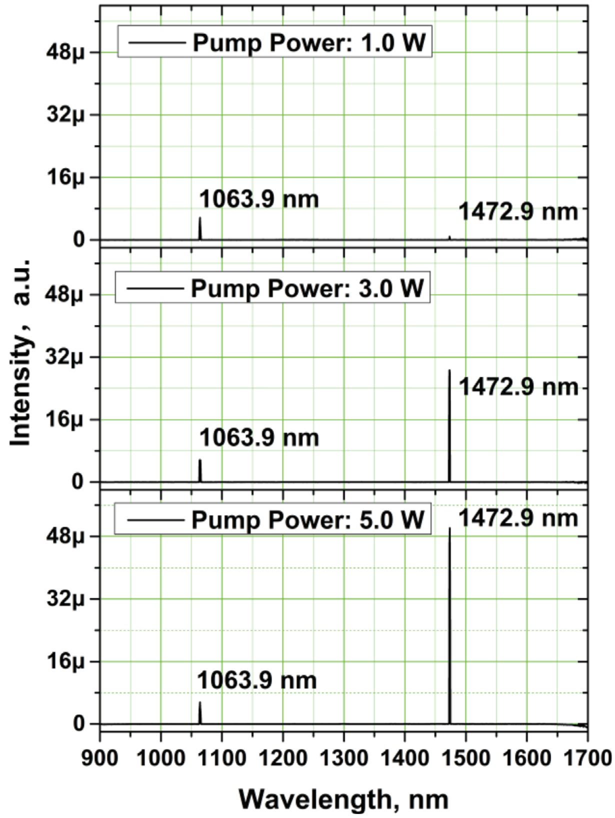

Figure 3. Output spectra of fundamental and signal lights under different pump powers (1.0, 3.0 and 5.0 W).

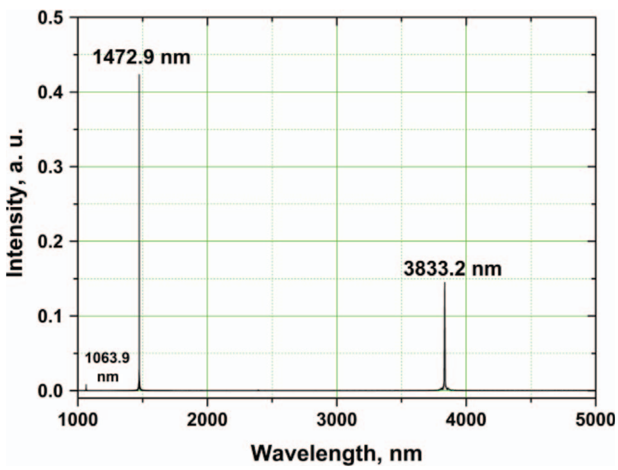

Figure 4. Output spectra of signal and idler lights at a pump power of 5.0 W.

is approximately 0.9 W. As the pump power at 807.6 nm increases, the signal and idler lights increase linearly. At the maximum pump power of 5.0 W, the power of the signal light and idler light reach 430 mW and 187 mW respectively; the total power is 617 mW. The total optical-to-optical conversion efficiency is 12.3%, and the conversion efficiency of the mid-infrared light at 3.8 μm is 3.7%. The slope efficiencies for the signal, idler, and total output power are 10.3%, 4.5%, and 14.8%, respectively.

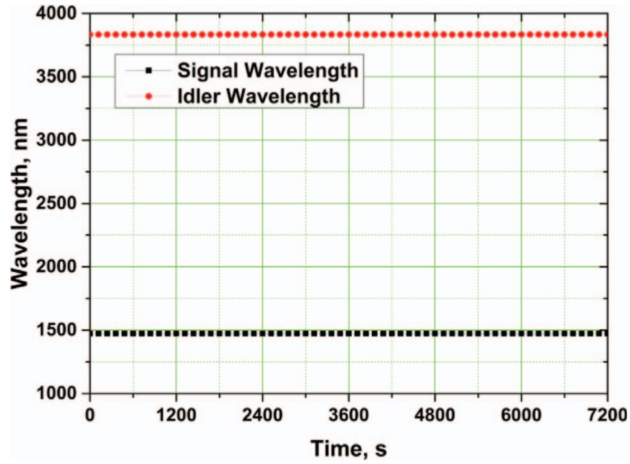

Figure 5. Wavelength stability of the signal and idler lights over two hours.

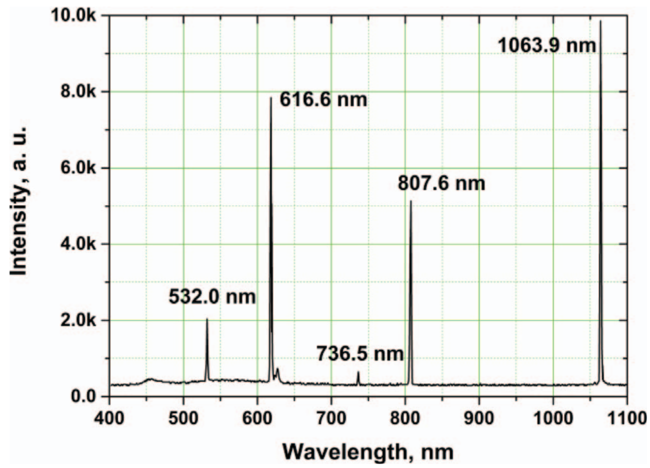

Figure 6. Output spectra of parasitic visible light, pump light, and signal light measured at a pump power of 5.0 W.

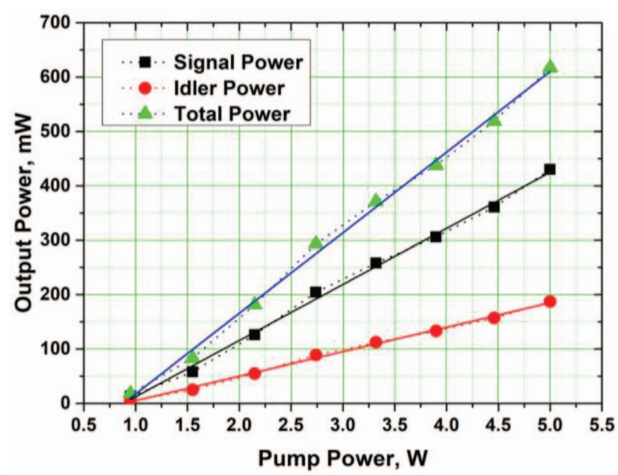

Figure 7. Output powers of the signal, idler, and total OPO as a function of pump power.

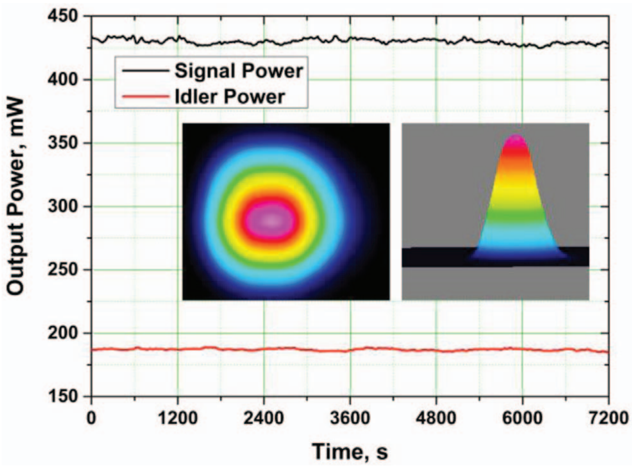

Figure 8. The power stability of the signal light and the idler light, and the output spot of the signal light.

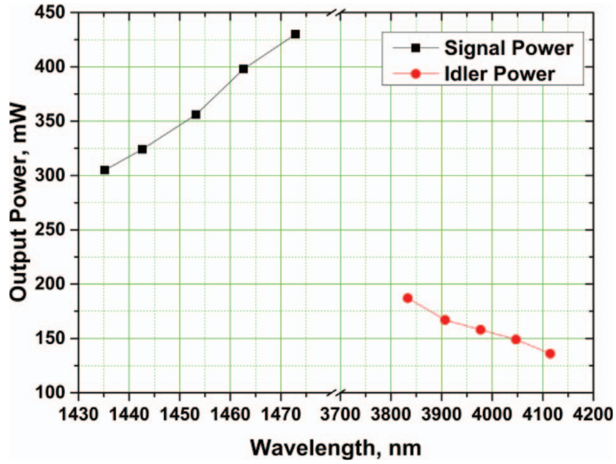

Figure 9. The output powers of the signal and idler lights at different wavelengths under 5.0 W pump power.

Table 1. Comparison of key performance parameters between the present shared-cavity OPO and previous works.

Structure	Oscillation threshold	Wavelengths	Output power	Efficiency	System dimensions	Reference
Intra-cavity	2.8 W	3.2 μm	410 mW	7.7%	> 140 mm	[7]
Intra-cavity	1.6 W	3.52 μm	65 mW	2.2%	/	[20]
Self-intra-cavity	> 8 W	3.86 μm	0.38 W	2.5%	> 128 mm	[9]
Intra-cavity	2 W	3.3 μm	1.32 W	7.2%	> 200 mm	[21]
Extra-cavity	1.86 W	3217 nm	1101.2 mW	12.5%	> 300 mm	[12]
Shared-cavity	6.9 W	1476.4 nm, no idler	580 mW	/	120 mm	[13]
Shared-cavity	0.9 W	3833.2 nm	187 mW	3.7%	70 mm	Here

Meanwhile, the output power stability of the signal light and the idler light is measured over a period of two hours, as shown in Figure 8, with power fluctuations of 2.6% and 1.5%, respectively. The stability of the signal light is slightly poorer, which is primarily caused by the parasitic oscillations in the visible light. The output beam spot of the signal light at 1472.9 nm is also shown in Figure 8, which is measured using a slit-scan beam profiler (Beam 'R2, DataRay Inc.). The output spot has good symmetry and an ellipticity of 0.98, along with a Gaussian energy profile. The M^2 factor is measured to be approximately 1.3. These results confirm the favorable performance of the shared-cavity structure, reflecting its high quality and proper alignment.

When the PPMgLN's periods are 28.6, 28.8, 29.0, 29.2 and 29.4 μm respectively, the idler powers of the mid-infrared wavelengths at 4114.8, 4046.9, 3977.2, 3907.0 and 3833.2 nm are 136, 149, 158, 167 and 187 mW under the 5.0 W pump power, respectively, as shown in Figure 9.

3.4 Performance comparison

To directly evaluate the performance of our shared-cavity OPO against state-of-the-art configurations, we summarize in Table 1 the key parameters of the present system together with those of representative previous works [7, 9, 12, 13, 20, 21]. As summarized in Table 1, the shared-cavity OPO presented in this work exhibits several distinct advantages over previously reported configurations. First, the oscillation threshold of 0.9 W is the lowest among all compared systems. Second, the total length of 70 mm is the most compact, which is enabled by eliminating separate pump coupling optics. Third, despite the simplicity of the design, the mid-IR output performance (187 mW at 3833.2 nm, 3.7% efficiency) is competitive with or better than many more complex systems. Our efficiency is competitive with those of reported intra-cavity and extra-cavity OPOs. The main limiting factors are round-trip + loss ≈4% (including 2% output coupling and 2% other losses), mode overlap integral ≈0.96, and parasitic nonlinear processes.

It is also important to note that both intra-cavity and extra-cavity configurations typically require multiple cavity mirrors and/or external coupling lenses, leading to larger footprints and more critical alignment procedures. In contrast, our shared-cavity architecture uses only two mirrors (M_{in} directly coated on the Nd:YVO_4 crystal and M_{oc} as the output coupler) and no additional beam-shaped optics. This inherent simplicity not only reduces the system size but also improves long-term stability and ease of operation.

4 Conclusion

This paper presents a mid-infrared OPO based on a shared cavity structure and a c-mount packaged LD pump source. This efficient design achieves good spatial mode self-consistency and cavity power enhancement of the fundamental and signal lights through a shared cavity, significantly improving the conversion efficiency. Meanwhile, the adoption of a shared cavity structure greatly reduces the complexity and cost of the OPO system, enabling a compact, economical and reliable integrated device. Using a low-power LD and a simple shared cavity structure, mid-infrared laser output can be achieved. Such a configuration not only maintains system miniaturization and operational simplicity but also expands the potential for applications in spectroscopy, sensing, and infrared imaging where tailored mid-infrared laser radiation is highly desirable.

The continuous-wave operation mode has limitations in peak power and transient detection capability. Therefore, future work will focus on the research of pulsed shared-cavity OPOs by adopting Q-switched or mode-locked structures, it is expected to obtain high peak power and narrow pulse width mid-infrared output while maintaining the high efficiency and stability of the shared-cavity structure. This direction is expected to further expand the application of the system in fields such as lidar, nonlinear spectroscopic imaging, and ultrafast detection. At the same time, exploring pulsed shared-cavity OPOs based on other nonlinear crystals (such as PPLT, PPKTA, ZGP, etc.) will also be an important way to achieve wider coverage of the mid-infrared band.

Funding

This paper was supported by the Natural Science Foundation of Xiamen City (3502Z202673045).

Conflicts of interest

The authors declare that there are no conflicts of interest.

Data availability statement

Data underlying the results presented in this paper are not publicly available at this time but may be obtained from the authors upon reasonable request.

Author contribution statement

Conceptualization, Yi-Ping Wang and Hong-Yi Lin; methodology, Yi-Ping Wang; validation, Shi-Chuang Jiang and Hong-Yi Lin; formal analysis, Yi-Ping Wang, Hong Liu and Hong-Yi Lin; investigation, Shi-Chuang Jiang, Dong Sun and Hong Liu; resources, Yi-Ping Wang, Liang-Qin Gang and Hong-Yi Lin; writing – original draft preparation, Yi-Ping Wang and Hong-Yi Lin; writing – review and editing, Dong Sun and Hong Liu; visualization, Liang-Qin Gan and Hong-Yi Lin; supervision, Dong Sun, Liang-Qin Gan and Hong-Kai Nian; project administration, Yi-Ping Wang and Hong-Kai Nian; funding acquisition, Yi-Ping Wang, Hong-Kai Nian and Hong-Yi Lin. All authors have read and agreed to the published version of the manuscript.

References

1 Chen WD, et al., Power scaling of tunable, narrowband, non-resonant PPLN optical parametric oscillators, *J. Eur. Opt. Society-Rapid Publ.* **22**, 4 (2026). https://doi.org/10.1051/jeos/2025052.

2 Wei XB et al., High-power mid-infrared ZGP optical parametric oscillator directly pumped by pulsed Tm:YLF laser at 1908 nm, *Opt. Laser Technol.* **161**, 109135 (2023). https://doi.org/10.1016/j.optlastec.2023.109135.

3 Wang H et al., A high-energy, long-wave infrared laser based on $ZnGeP_2$ optical parametric oscillator and amplifier, *Infrared Phys. Technol.* **145**, 105662 (2025). https://doi.org/10.1016/j.infrared.2024.105662.

4 Chen SY et al., Efficient 10 ns-scale 2-μm optical parametric oscillator based on 1064 nm pump source, *Front. Phys.* **12**, 1383254 (2024). https://doi.org/10.3389/fphy.2024.1383254.

5 Zhang JJ et al., 3 μm mid-infrared compact intracavity optical parametric oscillator based on KTA and MgO:PPLN, *Laser Phys. Lett.* **21**, 125004 (2024). https://doi.org/10.1088/1612-202X/ad8cc1.

6 Temel T et al., Power scaling of a narrowband-seeded, non-resonant optical parametric oscillator based on periodically poled $LiNbO_3$, *Photonics* **12**, 743 (2025). https://doi.org/10.3390/photonics12080743.

7 Lin HY et al., Mid-infrared, wide-tunable, continuous-wave Nd:YVO_4/PPMgLN intracavity optical parametric oscillator, *Optik* **125**, 6969–6971 (2014). https://doi.org/10.1016/j.ijleo.2014.08.053.

8 Yan RP et al., Investigation on 1.3 μm laser performance with Nd:$Gd_{0.69}Y_{0.3}TaO_4$ and Nd:$Gd_{0.68}Y_{0.3}NbO_4$ mixed crystals, *Opt. Express* **26**, 15785–15792 (2018). https://doi.org/10.1364/OE.26.015785.

9 Wei XB et al., Compact mid-infrared self-optical parametric oscillator directly-pumped by diode laser based on a single Nd:MgO:PPLN crystal, *Opt. Laser Technol.* **151**, 108062 (2022). https://doi.org/10.1016/j.optlastec.2022.108062.

10 He Y et al., High-power mid-infrared pulse MgO:PPLN optical parametric oscillator pumped by linearly polarized Yb-doped all-fiber laser, *Opt. Laser Technol.* **146**, 107545 (2022). https://doi.org/10.1016/j.optlastec.2021.107545.

11 Abulikemu A et al., Mid-infrared idler-resonant optical vortex parametric oscillator based on MgO:PPLN, *Opt. Laser Technol.* **171**, 110341 (2024). https://doi.org/10.1016/j.optlastec.2023.110341.

12 Lin HY et al., Extra-cavity, widely tunable, continuous wave MgO-doped PPLN optical parametric oscillator pumped with a Nd:YVO_4 laser, *Opt. Mater.* **32**, 257–260 (2009). https://doi.org/10.1016/j.optmat.2009.07.019.

13 Lin HY et al., Continuous-wave eye-safe Nd:YVO_4/PPMgLN intra-cavity optical parametric oscillator with shared resonator, *Optik* **138**, 127–129 (2017). https://doi.org/10.1016/j.ijleo.2017.03.061.

14 Zhang CB et al., Measurement of the laser diode end-pumped solid laser's thermal focal length by using the curve of output, *Acta Phys. Sin.* **51**, 1517–1520 (2002). https://doi.org/10.7498/aps.51.1517.

15 Liu JH et al., Thermal lens determination of end-pumped solid-state lasers by a simple direct approach, *Chin. Phys.*

Lett. **16**, 181–182 (1999). https://doi.org/10.1088/0256-307X/16/3/010.

16 Sennaroglu A, Experimental determination of fractional thermal loading in an operating diode-pumped Nd:YVO_4 minilaser at 1064 nm, *Appl. Opt.* **38**, 3253–3257 (1999). https://doi.org/10.1364/AO.38.003253.

17 PPMgLN parameters, Shalom EO (2026). https://www.shalomeo.com/index.php?path=223_424&product_id=1908&route=product/product (accessed 30 April 2026).

18 Lin HY et al., Parasitic oscillation in mid-infrared optical parametric generator based on PPMgLN, *Optik* **124**, 2511–2513 (2013). https://doi.org/10.1016/j.ijleo.2012.08.027.

19 Segur F et al., Parasitic photon analysis in sum frequency generation using a bulk PPLN crystal, *J. Eur. Opt. Society-Rapid Publ.* **21**, 46 (2025). https://doi.org/10.1051/jeos/2025044.

20 Carleton A et al., Compact, continuous-wave, singly resonant optical parametric oscillator based on periodically poled $RbTiOAsO_4$ in a Nd:YVO_4 laser, *Opt. Lett.* **28**, 555–557 (2003). https://doi.org/10.1364/OL.28.000555.

21 Chen BT et al., Low-threshold dual-wavelength CW mid-IR laser from shared intracavity quasi-phase-matched OPO, *Opt. Lett.* **48**, 1770–1773 (2023). https://doi.org/10.1364/OL.486183.